CONF-960804--36 ANL/CMT/CP--89778

STAINLESS STEEL-ZIRCONIUM ALLOY WASTE FORMS FOR METALLIC FISSION PRODUCTS AND ACTINIDES ISOLATED DURING TREATMENT OF SPENT NUCLEAR FUEL*

Sean M. McDeavitt
Argonne National Laboratory
9700 South Cass Avenue
Argonne, Illinois 60439
(708) 252-4308

Daniel P. Abraham
Argonne National Laboratory
9700 South Cass Avenue
Argonne, Illinois 60439
(708) 252-5486

Dennis D. Keiser, Jr.
Argonne National Laboratory
P.O. Box 2528
Idaho Falls, Idaho 83403
(208) 533-7298

Jang-Yul Park
Argonne National Laboratory
9700 South Cass Avenue
Argonne, Illinois 60439
(708) 252-5030

To Be Presented At:
SPECTRUM '96
Seattle, Washington, USA
August 18-23, 1996

*Work supported by the U.S. Department of Energy, Nuclear Energy Research and Development Program, under Contract No. W-31-109-Eng. 38.

DISCLAIMER

STAINLESS STEEL-ZIRCONIUM ALLOY WASTE FORMS FOR METALLIC FISSION PRODUCTS AND ACTINIDES ISOLATED DURING TREATMENT OF SPENT NUCLEAR FUEL

Sean M. McDeavitt
Argonne National Laboratory
9700 South Cass Avenue
Argonne, Illinois 60439
(708) 252-4308

Daniel P. Abraham
Argonne National Laboratory
9700 South Cass Avenue
Argonne, Illinois 60439
(708) 252-5486

Dennis D. Keiser, Jr.
Argonne National Laboratory
P.O. Box 2528
Idaho Falls, Idaho 83403
(208) 533-7298

Jang-Yul Park
Argonne National Laboratory
9700 South Cass Avenue
Argonne, Illinois 60439
(708) 252-5030

ABSTRACT

Stainless steel-zirconium waste form alloys are being developed for the disposal of metallic wastes recovered from spent nuclear fuel using an electrometallurgical process developed by Argonne National Laboratory. The metal waste form comprises the fuel cladding, noble metal fission products, and other metallic constituents. Two nominal waste form compositions are being developed: (1) stainless steel-15 wt% zirconium for stainless steel-clad fuels and (2) zirconium-8 wt% stainless steel for Zircaloy-clad fuels. The noble metal fission products are the primary source of radiation and their contribution to the waste form radioactivity has been calculated. The disposition of actinide metals in the waste alloys is also being explored. Simulated waste form alloys were prepared to study the baseline alloy microstructures and the microstructural distribution of noble metals and actinides, and to evaluate corrosion performance.

I. INTRODUCTION

Alloy waste forms are being developed at Argonne National Laboratory for the immobilization of metallic materials left behind following the electrometallurgical treatment of spent nuclear fuel.[1-4] This treatment process is being implemented as a full-scale demonstration in the Fuel Conditioning Facility (FCF)[5] in conjunction with the shutdown and dismantling of the Experimental Breeder Reactor-II (EBR-II). The principal step in this process is the electrorefining of uranium metal in a molten salt electrolyte.[6-7] Three distinct material streams emanate from the electrorefiner: (1) refined metallic uranium; (2) fission products and actinides extracted from the electrolyte salt that are processed into a mineral waste form; and (3) metallic wastes that are consolidated into the metal waste form.

The metal waste form comprises the spent fuel cladding, the noble metal fission products (NMFP) (e.g., Ru, Rh, Pd, Zr, and Tc) that do not dissolve in the electrolyte salt, and, in some cases, zirconium metal from alloy nuclear fuels. These metallic wastes are not generated in the electrorefiner; they are present with the spent fuel before treatment. The spent fuel cladding hulls and NMFPs are inert in the electrorefiner environment and, therefore, remain in the charge basket as the uranium, other actinides, and active fission products are electrochemically dissolved or transported.

The term "waste form" refers to radioactive materials and any encapsulating or stabilizing matrix that will be placed into a "waste package" for disposal. The radioactive materials may be stabilized for disposal by encapsulation, chemical transformation, and/or inclusion in a stable matrix material. Vitrification in borosilicate glass has been widely selected as a primary stabilization method for high level wastes.[8] However, at least two issues make vitrification an undesirable option for the metallic waste stream considered here. First, NMFPs are strong crystal formers in vitrified waste forms and crystal formation decreases the mechanical integrity of glass.[9] Second, vitrification of the metallic wastes would result in very significant mass and volume increases. Minimizing the waste form volume is critical because the unit volume cost for repository disposal is expected to be quite high.

Two types of fuel were used in EBR-II: driver fuel and blanket fuel.[10] The driver fuel is a U-10 wt% Zr alloy[a] with Type 316 and D9 stainless steel cladding, and the blanket fuel is uranium metal with Type 304 stainless steel cladding. The cladding materials plus the NMFP and Zr from the driver fuel will be melted together into a uniform, corrosion-resistant alloy waste form. Approximately 0.5 to 4 wt % NMFP will be present in

[a] All compositions are in wt% unless indicated.

the metal waste form, depending on the fuel burnup. The alloying process will be carried out in a high-temperature, controlled-atmosphere melting furnace. A molten salt flux may be used as a solvent to dissolve residual electrolyte salt and maintain metal purity.

Although EBR-II fuel will be treated first, other spent fuels with stainless steel and Zircaloy claddings are being evaluated for future treatment. In all cases, the cladding hulls represent over 85% of the metal waste stream. By using the hulls as the major alloying component, the total waste form volume is minimized. This approach gave rise to the parallel development of two metal waste form compositions: (1) stainless steel-15 wt % zirconium (SS-15Zr) for stainless steel-clad fuel and (2) Zircaloy-8 wt% stainless steel (Zr-8SS) for Zircaloy-clad fuel. The metal waste form development effort includes the ongoing evaluation of the physical metallurgy, corrosion performance, thermophysical properties, and process variables important to waste form generation and qualification. Metal waste forms containing actinide metals[4] are also of interest as a backup option to the actinide-bearing mineral waste form.

II. METAL WASTE FORM ALLOYS

The nominal alloy compositions SS-15Zr and Zr-8SS were selected on the basis of initial characterization and corrosion data. In addition, such parameters as alloying temperature and minimal nonwaste additions were also considered. The SS-15Zr composition is near a eutectic having a melt temperature of ~1330°C. The Zr-8SS composition is not near a eutectic, but its liquidus temperature is ~1500°C. Therefore, both alloys may be produced at temperatures near 1600°C. A large-scale tilt-pour casting furnace (3 kg capacity) was designed, built, and connected to an inert atmosphere glovebox for use in developing the waste form alloying procedures. This furnace is being used to generate large ingots and to test processing parameters.

Small-scale (~20 g) stainless steel-zirconium alloys were generated that had a range of zirconium compositions to simulate the SS-15Zr and Zr-8SS waste forms and other SS-Zr alloy compositions.[2] The alloys were prepared from stainless steel (Types HT9, 304, or 316), zirconium, and selected noble metals (i.e., Ru, Pd, Mo, and Ag) that were melted at 1600°C in yttria (Y_2O_3) crucibles under an argon atmosphere for 1-2 h and solidified by cooling slowly. The microstructural evolution and phase development of SS-Zr alloys with various Zr contents was studied by using a scanning electron microscope (SEM), energy dispersive X-ray analysis (EDX), and X-ray diffraction.[2] More recently, neutron diffraction has been used to characterize phases that have only a minor presence in the waste form alloys.

Stainless steel-rich alloys containing 5 to 40 wt% Zr exhibit varying proportions of an iron solid solution phase and a Laves-type intermetallic (AB_2 crystal structure) that we have designated $Zr(Fe,Cr,Ni)_{2+x}$.[2] The microstructure of the nominal waste form for stainless steel-clad fuel, SS-15Zr, is presented in Figure 1. As a first approximation, the SS-15Zr alloy contains a

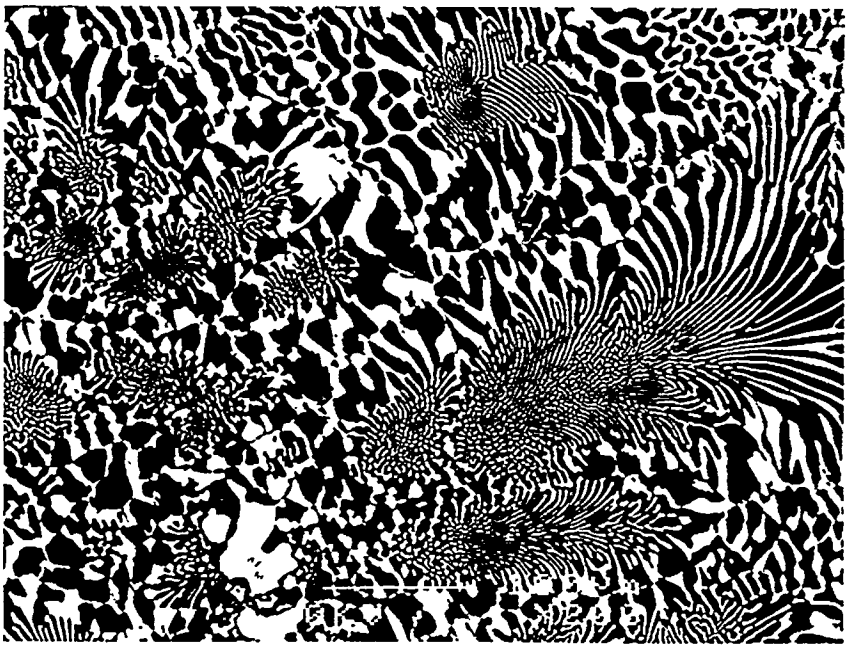

Figure 1. Backscattered Electron Image (200x) of the SS-15Zr Eutectic Structure. The dark phase is an iron solid solution, and the bright phase is the $Zr(Fe,Cr,Ni)_{2+x}$ intermetallic.

Table 1. Composition of Observed Phases in SS-15Zr and Zr-8SS Alloys.*

	Phase	Crystal Structure	Fe	Zr	Cr	Ni
SS-15Zr	α-Fe	BCC	69	0	24	4
	γ-Fe	FCC	70	0	20	8
	$Zr(Fe,Cr,Ni)_{2+x}$	AB_2 Laves phase	54	24	8	11
	Zr_6Fe_{23}-Type	Th_6Mn_{23}-Type	57	19	10	9
Zr-8SS	α-Zr	HCP	3	94	1.5	0.5
	$Zr(Fe,Cr)_2$	AB_2 Laves phase	42	34	21	0
	$Zr_2(Fe,Ni)$	$CuAl_2$-Type	28	66	0	6

* Listed compositions are in atom % (±3%).

two-phase structure, where the dark phase is a ferritic Fe (α-Fe) solid solution and the bright contrast phase is the intermetallic compound $Zr(Fe,Cr,Ni)_{2+x}$. The compositions of the various SS-15Zr alloy phases are given in Table 1.

Below ~15 wt% Zr, the Fe solid solution phase is found to be a mixture of α-Fe and austenitic Fe (γ-Fe), both of which contain Cr and Ni levels corresponding to those of ferritic and austenitic stainless steels.[2] A minor volume fraction of the γ-Fe phase is observed in SS-15Zr alloys generated with Type 316 stainless steel, whereas only the α-Fe phase is present when Type 304 stainless steel is used. This minor difference in structure is the result of a higher nickel content in Type 316 stainless steel vs. Type 304 stainless steel. The $Zr(Fe,Cr,Ni)_{2+x}$ intermetallic is a strong sink for Ni, an austenite stabilizer, but it saturates at low Zr concentrations, leaving excess Ni to stabilize the γ-Fe phase. The relative proportion of $Zr(Fe,Cr,Ni)_{2+x}$ increases with increasing zirconium concentration until ~40 wt% Zr, when the alloy is ~100% intermetallic and brittle. In addition, a minor quantity of a second intermetallic phase was identified by neutron diffraction and then observed using the SEM. This phase was identified as Zr_6Fe_{23}, a stable Fe-Zr intermetallic phase.[11]

Zirconium-rich alloys (>40 wt% Zr) contain multi-phase mixtures of various brittle intermetallic phases up to ~84 wt% Zr (16 wt% SS).[2] As the Zr content increases from 84 to 100 wt%, a zirconium solid solution phase (α-Zr) is observed in increasing quantity, along with decreasing quantities of the intermetallic phases. Figure 2 shows the microstructure of Zr-8SS, the nominal waste form alloy for Zircaloy-clad fuel. The Zr-8SS alloy possesses a multi-phase microstructure dominated by the primary α-Zr solid solution surrounded by a complex eutectic structure containing the α-Zr phase

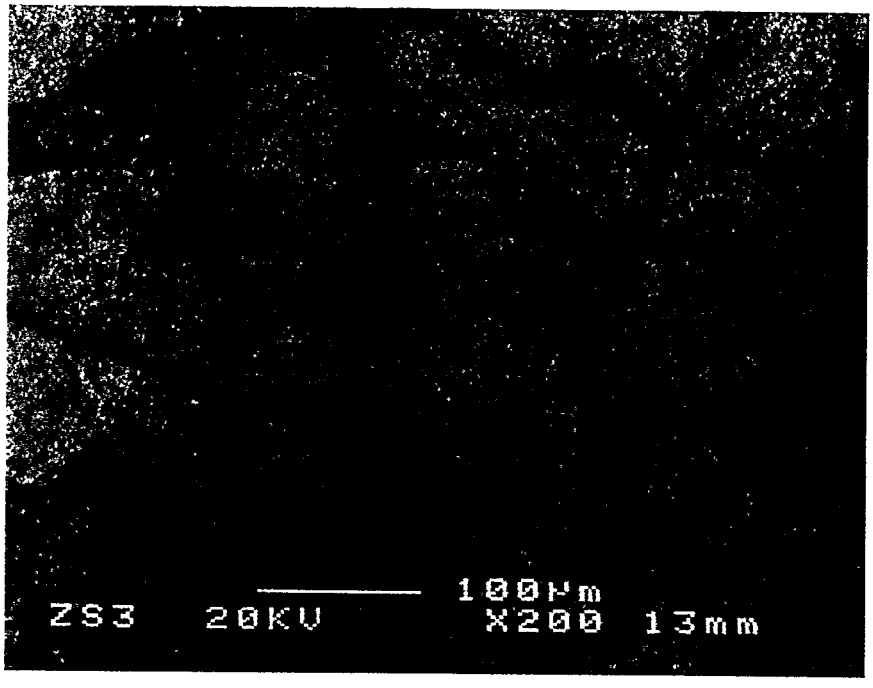

Figure 2. Backscattered Electron Image (200x) of the Zr-8SS Structure. The major phase is a zirconium solid solution, and the darker phases are intermetallics.

Table 2. Chemical Inventory and Radioactive Source Strength for EBR-II Metal Waste Stream

		Calculated 1996 Levels				Calculated Levels After 1000 y Decay			
		Mass (kg)	wt%	Activity (Ci)	Ci %	Mass (kg)	wt%	Activity (Ci)	Ci %
Zirconium	Fuel*	64	1.5	1.0×10^4	4.1	91	2.0	5.1	6.6
	Added	615	13.5	•	•	615	13.5	•	•
Cladding Components	Fe*	2300	50.8	1.6×10^4	6.5	2300	50.4	•	•
	Cr*	690	15.3	•	•	690	15.2	•	•
	Ni*	730	16.1	•	•	730	16.0	6.7	8.8
	Mo*	25	0.6	•	•	25	0.6	4.3	5.6
	Mn*	37	0.8	1.0×10^4	4.2	37	0.8	•	•
	Si*	19	0.4	•	•	19	0.4	•	•
	Co*	9	0.2	2.3×10^3	0.9	9	0.2	•	•
NMFP Elements	Ag	0.3	0.01	•	•	0.3	0.01	•	•
	Nb	6.1	0.14	2.3×10^4	9.3	6.1	0.13	12.9	16.9
	Pd	3.3	0.07	•	•	3.3	0.07	0.3	0.4
	Rh	2.1	0.05	8.8×10^4	35.7	2.1	0.05	•	•
	Ru	6.6	0.15	8.8×10^4	35.7	6.6	0.14	•	•
	Sb	0.06	0.00	8.4×10^3	3.4	0.05	0.00	3.0	4.0
	Sn	0.2	0.01	4.5×10^2	0.2	0.2	0.01	2.7	3.5
	Ta	0.9	0.02	•	•	0.9	0.02	•	•
	Tc	2.5	0.05	•	•	2.4	0.05	41.4	54.2
NMFP Totals†		22	0.49	2.2×10^5	88.4	22	0.49	65.4	85.6
Column Totals		4511	99.7	2.5×10^5	100	4538	99.6	76.4	100

* Numbers include minor quantities of NMFP, activation product, and/or decay product isotopes.
† NMFP activity totals include numbers from fuel Zr.
• Activity either zero or orders of magnitude below dominant radioactive species.

and intermetallic compounds; these intermetallics have been qualitatively identified as $Zr_2(Fe,Ni)$ and $Zr(Fe,Cr)_2$. The compositions of the Zr-8SS alloy phases are presented in Table 1.

III. NOBLE METAL FISSION PRODUCTS

The fission product composition in spent nuclear fuel is dependent upon the fuel's accumulated burnup. That is, as nuclear fission occurs, the fuel isotopes (e.g., U-235) split into a wide variety of lighter isotopes. The entire fission product inventory includes gases and chemically active isotopes that are not included in the metal waste stream. NMFPs represent ~35% of the total fission product inventory. The actual quantity and composition of NMFPs present in a given metal waste stream are dependent on starting fuel composition, neutron energy spectrum, and the duration of irradiation.

A nuclear fuel modeling code, ORIGEN, was used to calculate the fission product inventory of EBR-II fuel[b] in its current state and at future times by simulating changes due to radioactive decay. The data listed in Table 2 represent the chemical inventory (in kg) and radioactivity (in Curies) of the EBR-II metal waste stream. The values listed are combined totals for Mark-III driver fuel and blanket fuel. The NMFP content in the driver fuel is expected to be as high as 2 to 4 wt%, whereas the NMFP content in the blanket is expected to be below 0.5 wt%. The zirconium data was separated to distinguish between Zr from the spent fuel and non-reactor Zr that will be used to generate the SS-15Zr alloy. Several minor cladding components and impurities (e.g., C, Ti, and Cu) and NMFPs (e.g., Cd, In, V, and Zn) are not included in Table 2. (The missing cladding materials account for the 0.3 wt% deficit in the second column, whereas the missing NMFPs represent <0.01 wt% of the entire inventory.)

Each element listed in Table 2 is present as several different isotopes, and the intense initial radioactivity comes from NMFP isotopes present in very minor concentrations. The metal waste form composition is, therefore, not significantly altered as the high-activity, short-lifetime isotopes decay away. For example, ORIGEN predicts ~6.6 kg of Ru in EBR-II fuel, but the ~88,000 Ci initial activity comes exclusively from an estimated 0.3 g of Ru-106 and Ru-103, which have half-lives of 372.6 d and 39.2 d, respectively.

The intense initial radioactivity decays rapidly as transmutation occurs. Figure 3 shows the time-dependent

[b] Calculation by R. N. Hill, Reactor Analysis Division, Argonne National Laboratory.

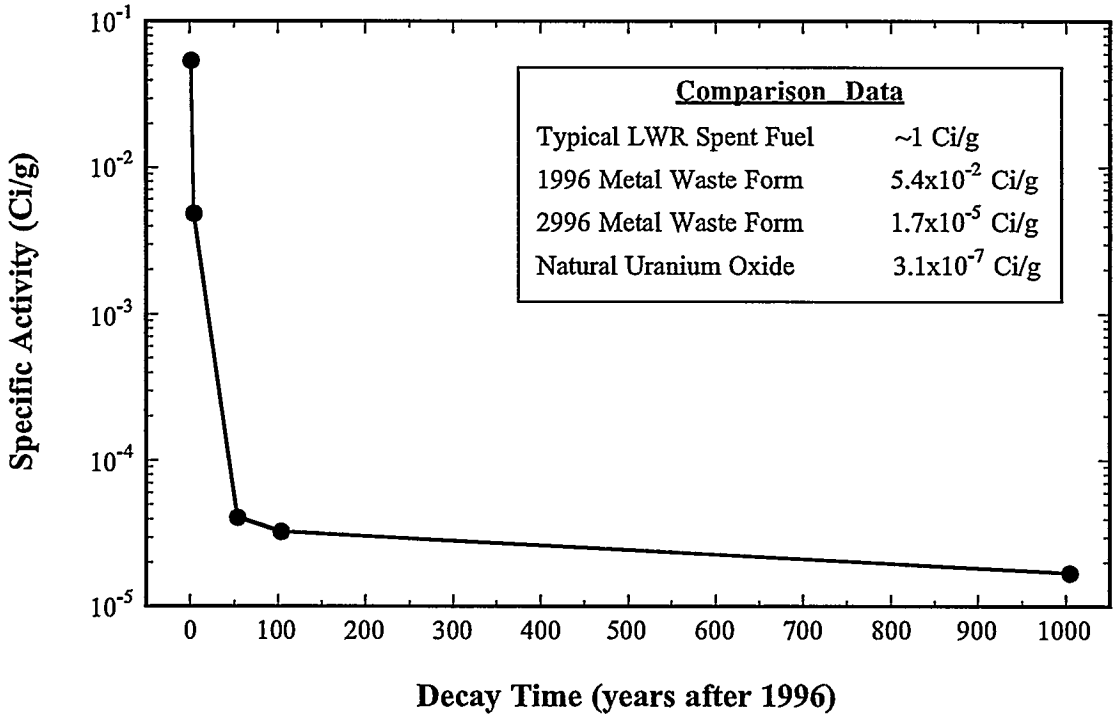

Figure 3. Calculated Specific Activity of EBR-II Metal Waste Form vs. Time.

change in specific activity for an "average" EBR-II metal waste form (i.e., Table 2 composition). The radiation level drops precipitously over the first 100 years and settles into a long-term rate of decay dominated by long-lived NMFP isotopes, primarily Tc-99. The metal waste form activity is relatively benign when compared to spent light water reactor (LWR) fuel and other radioactive waste forms that may be permanently disposed of in a geologic repository. ORIGEN calculations[b] indicate that the long-term specific activity of typical LWR spent fuel is on the order of 1 Ci/g, even after 10^6 years. The EBR-II metal waste form activity will be only ~0.05 Ci/g at its peak, and it decays rapidly to ~$3x10^{-5}$ Ci/g in the first 100 y. This value is only two orders of magnitude higher than the specific activity of natural uranium oxide.

The noble metals Ru, Re, Pd, Mo, and Ag were added experimentally to SS-15Zr and Zr-8SS alloy samples to simulate the presence of NMFPs, and the total nobl metal content ranged from 1 to 5 wt% (a typical addition to SS-15Zr was 2 Ru-1.5 Pd-0.5 Ag). Alloy microstructures were examined, and discrete noble metal phases were not observed. No differences were seen between noble metal-containing microstructures and the baseline microstructures (e.g., Figures 1 and 2). For SS-15Zr alloys, the noble metals were dissolved and distributed between the intermetallic and the iron solid solution phase. Some elements (i.e., Ru, Pd, and Ag) showed a ~2:1 preference for the intermetallic phase, while others (i.e., Re) showed a similar preference for the iron solution phase. The noble metal distribution has not yet been quantified for the Zr-8SS alloy, but a similar absence of noble metal precipitation was seen. These observations indicate that the stainless steel-zirconium waste form alloys are indeed viable as NMFP disposition alloys.

IV. ACTINIDE-BEARING WASTE FORMS

Small-scale samples of simulated waste form alloys (~30 g) containing U, Pu, and Np were generated by melting in yttria crucibles at 1600°C for 2 h under a flowing argon atmosphere and cooling slowly to room temperature. The samples included SS-15Zr alloys with actinide compositions of 0.5U-0.5Pu, 2U-2Pu, 6Pu, 10Pu, 6Pu-2Np, and 2Np and Zr-8SS alloys with 4, 7, and 10 wt% Pu. The SS-15Zr alloys were generated using Type 316 stainless steel, and the Zr-8 stainless steel alloys were generated using Type 304 stainless steel. The high actinide concentrations used in this study were selected to provide insight into the actinide interactions with the existing phases. If actinides are placed into the metal waste form in actual practice, the concentration will be between 1 and 10 wt%.

Figure 4 presents a representative microstructure for the actinide-bearing SS-15Zr alloys that is similar to the baseline SS-15Zr microstructure in Figure 1. There is 2 atom % Pu in the $Zr(Fe,Cr,Ni)_{2+x}$ intermetallic, but no actinides are detectable in the iron solid solution phase.

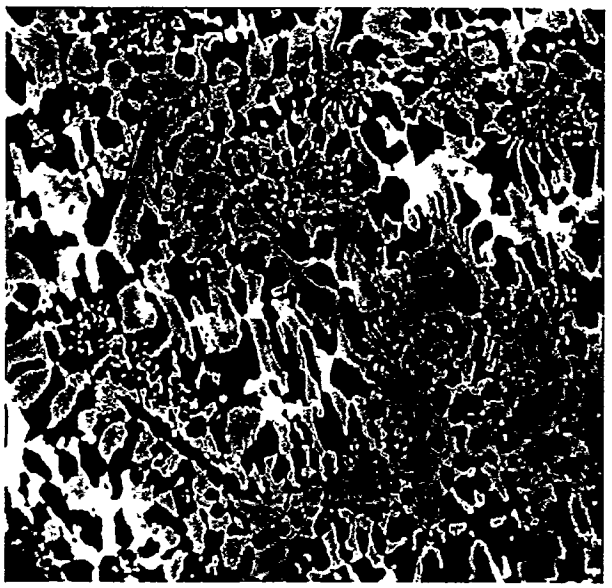

Figure 4. Backscattered Electron Image of SS-15Zr Alloy Containing 2 wt% U and 2 wt% Pu. The bright contrast phases are rich in U and Pu.

The high-contrast phase is an intermetallic that is apparently miscible with the $Zr(Fe,Cr,Ni)_{2+x}$ phase; its composition is 33 atom % Fe-33 atom % Ni-20 atom % actinide (U, Pu, and/or Np) plus small amounts of Zr and Cr. This phase was observed in all of the actinide-bearing SS-15Zr alloys, irrespective of the actinide or group of actinides included in the sample; increasing the actinide content resulted in a higher volume fraction of this phase. Additionally, changes in the zirconium content of the $Zr(Fe,Cr,Ni)_{2+x}$ phase were observed in Np-bearing alloys. The Zr content was as low as 13 atom % in the sample with 2 atom % Np. For actinide-bearing alloys without Np, the Zr content in the $Zr(Fe,Cr,Ni)_{2+x}$ phase was ~22 atom %, similar to the 24 atom % reported for the baseline alloy in Table 1. The Fe solid solution phase did not exhibit any concentration differences.

Figure 5 presents a representative microstructure for the Zr-8SS-xPu alloys. Again, the microstructure

Figure 5. Backscattered Electron Image of Zr-8SS Alloy Containing 10 wt% Pu (300x). The bright-contrast features are α-Zr phase boundaries with ~12 atom % Pu.

resembles the corresponding baseline alloy (Figure 2). The Pu was observed in solution in the α-Zr metal matrix, but it was also found in higher concentrations at the α-phase boundaries (i.e., the bright spike-like features in Figure 5). The formation of these Pu-rich features may be explained as follows: (1) the high-temperature zirconium metal phase, β-Zr, is completely miscible with the high-temperature plutonium metal phase, ε-Pu, but the low-temperature zirconium metal phase, α-Zr, has limited solubility for plutonium (<13 atom %); (2) the β-Zr metal forms first upon cooling, with up to 100% of the plutonium in solution; (3) β-Zr transforms to α-Zr at ~863°C; and (4) the excess Pu that exceeds α-Zr solubility becomes concentrated at newly formed α-Zr phase boundaries. Increasing the amount of Pu added to the alloy from 4 to 10 wt% Pu resulted in higher amounts of Pu both in the α-Zr matrix phase (from 1.5 to 5 atom % Pu) and at the α-phase boundaries (up to 12 atom % Pu).

Neither actinide-bearing alloy exhibits pure actinide phases. Since the actinides are entrained in complex, but stable, matrix phases, the stainless steel-zirconium alloy waste forms have potential application as actinide disposal alloys. Performance testing must be carried out in the future to verify this viability, but since Pu has only a minor effect on the alloy microstructure, the performance of the baseline alloys (discussed in Section V) may be used to infer the performance of the actinide-bearing alloys.

V. WASTE FORM EVALUATION

Small-scale samples with various zirconium contents were machined and polished into disks and tested using general immersion and electrochemical corrosion methods. Large-scale ingots made in the 3 kg-capacity tilt-pour furnace were used to generate specimens for testing corrosion, mechanical, and thermophysical properties. Preliminary data indicate that the SS-15Zr alloy is a very strong metal with minimal tensile ductility. Uniaxial tension tests on specimens revealed elongation of <1% and a fracture strength on the order of 40 ksi.

Corrosion resistance is the primary performance indicator for the metal waste form. Corrosion testing was typically carried out using simulated J-13 well water, which is representative of the groundwater at the Yucca Mountain site in Nevada that has been proposed for a high-level nuclear waste repository. The ionic concentration of J-13 well water is (in mg/L): 11.5 Ca, 1.76 Mg, 45.0 Na, 5.3 K, 0.06 Li, 0.04 Fe, 0.001 Mn, 0.03 Al, 30.0 Si, 2.1 F^-, 6.4 Cl^-, 18.1 SO_4^{2-}, 10.1 NO_3^-, 143.0 HCO_3^-, and 5.7 dissolved oxygen.

General immersion corrosion tests were carried out using a test procedure based on the MCC-1 Static Leach Test developed for glass-based waste forms. Disk specimens, 15.9 mm diameter and 3 mm thick, were polished to a 600 grit finish, immersed in the J-13 solution in a sealed Teflon vessel, and placed in an oven at 90°C. Test specimens made from SS-15Zr and Zr-8SS alloys and other off-nominal Zr compositions were tested. However, the test solution was benign to the stainless steel-zirconium alloys, and corrosion rates were not measurable. In fact, most of the surfaces of the immersion specimens remained shiny after exposure durations up to 10,000 h (381 d). This is a positive result, but it does not provide a quantitative means to evaluate the waste form performance.

Another test method employed is the electrochemical linear polarization measurement of corrosion rates. This method can measure very low corrosion rates in a short duration test. The electrochemical cell current is measured and mathematically converted into a uniform corrosion rate; localized corrosion may affect this measurement, but we have not observed any evidence of this phenomena. Measurements were made at pH = 2, 4, 7, and 10 to cover a range of potential repository conditions; pH = 2 represents an extreme acidic condition that may not occur in the repository environment, but it provides an aggressive test to compare the relative performance of these low-corrosion-rate metals.

The electrochemical corrosion rates are shown in Table 3 for the waste form alloys, commercial zirconium and stainless steel, and selected candidate canister materials. The waste form corrosion rates at pH = 7 are comparable or slightly lower than the measured rates for Types 316 and 304 stainless steel and zirconium metal. Noble metal additions do not significantly affect the corrosion rates of the waste form alloys. Also, the measured waste form corrosion rates are similar to the rate for Incoloy 825, lower than the rate for pure copper, and two orders of magnitude lower than the rate for mild steel.

VI. SUMMARY

Stainless steel-zirconium alloy waste forms are being developed for the remnant metallic wastes from the electrometallurgical treatment of spent nuclear fuel. The alloys SS-15Zr and Zr-8SS are the baseline waste form alloys for stainless steel-clad and Zircaloy-clad fuels, respectively. The microstructures of these alloys were characterized to provide data for the evaluation of NMFP and actinide inclusion. The NMFPs from the spent fuel are present in small quantities and are distributed in solid solution. Corrosion tests have shown that the metal waste form alloys are highly corrosion resistant, both with

Table 3. Electrochemical Corrosion Rates of Waste Form and Waste Canister Alloys

Alloy (in wt%)	Corrosion Rates (MPY*) pH=2	pH=4	pH=7	pH=10
SS-15Zr	0.1-0.4	0.08-0.2	0.02-0.08	0.01-0.02
SS-15Zr-2Ru-1.5Pd-0.5Ag	0.4-0.5	0.2	0.04-0.1	0.06-0.09
Zr-8SS	0.02-0.08	0.05-0.06	0.02-0.03	0.01
Zr-8SS-1Ru-1Mo-0.5Pd	0.08	0.04	0.03	0.01
Zirconium	0.02	0.1	0.06-0.09	0.07
Type 304 SS	0.1	0.05	0.05	0.03
Type 316SS	0.3	0.05	0.04	0.03
Incoloy 825	0.03	0.05	0.07	0.03
Cu-7Al (CDA614)	2.3	6.9	3.6	2.0
A106 Grade B low alloy steel	50	23	12	12

* MPY = mils per year. Number ranges indicate multiple measurements.

and without the presence of NMFPs. Actinides slightly modify the phase structure of the alloys, but data is not yet available regarding the effects on corrosion performance.

ACKNOWLEDGMENTS

The authors would like to acknowledge J. K. Basco and P. A. Hansen for their supporting efforts in this work. This work was supported by U. S. Department of Energy under contract W-31-109-Eng-38.

REFERENCES

1. S. M. McDeavitt, J. Y. Park, and J. P. Ackerman, "Defining a Metal-Based Waste Form for IFR Pyroprocessing Wastes," *Actinide Processing: Methods and Materials*, eds. B. Mishra and W.A. Averill, p. 305-319, The Minerals, Metals, & Materials Society, Warrendale, Pennsylvania (1994).

2. D. P. Abraham, S. M. McDeavitt, and J. Y. Park, "Microstructure and Phase Identification in Type 304 Stainless Steel-Zirconium Alloys," Accepted for publication in *Metall. and Mater. Trans.* (1996).

3. D. P. Abraham, S. M. McDeavitt, and J. Y. Park, "Metal Waste Forms From The Electrometallurgical Treatment of Spent Nuclear Fuel," *Proc. DOE Spent Nuclear Fuel & Fissile Material Management*, Reno, Nevada, June 16-20, 1996, American Nuclear Society, LaGrange Park, Illinois (1996).

4. D. D. Keiser, Jr. and S. M. McDeavitt, "Actinide-Containing Metal Disposition Alloys," *Proc. DOE Spent Nuclear Fuel & Fissile Material Management*, Reno, Nevada, June 16-20, 1996, American Nuclear Society, LaGrange Park, Illinois (1996).

5. J. E. Battles, J. J. Laidler, C. C. McPheeters, and W. E. Miller, "Pyrometallurgical Process for Recovery of Actinide Elements," *Actinide Processing: Methods and Materials*, eds. B. Mishra and W.A. Averill, p. 135-151, The Minerals, Metals, & Materials Society, Warrendale, Pennsylvania (1994).

6. E. C. Gay and W. E. Miller, "Electrorefining N Reactor Fuel," *Proc. DOE Spent Nuclear Fuel Challenges and Initiatives*, Salt Lake City, Utah, Dec. 13-16, 1994, p. 267, American Nuclear Society, LaGrange Park, Illinois (1994).

7. J. P. Ackerman, "Chemical Basis for Pyrochemical Reprocessing of Nuclear Fuel," *Ind. Eng. Chem. Res.*, **30**, 29 (1991).

8. A. J. G. Ellison, J. J. Mazer, and W. L. Ebert, *Effect of Glass Composition on Waste Form Durability: A Critical Review*, Argonne National Laboratory Report ANL-94/28 (1994).

9. *High-Level Waste Borosilicate Glass, A Compendium of Corrosion Characteristics*, ed. J. J. Cunnane, Vol. 1, U.S. Department of Energy Report DOE-EM-0177 (1994).

10. L. C. Walters, B. R. Seidel, and J. H. Kittel, "Metallic Fuels and Blankets in LMFBRs," *Nuclear Technology*, **65**, 179 (1984).

11. Y. Liu, S. M. Allen, and J. D. Livingston, "An Investigation of Fe_3Zr Phase," *Scripta Metallurgica et Materialia*, **32**, 1129 (1995).